MULTI-TARGET MOTION PARAMETER ESTIMATION EXPLOITING COLLABORATIVE UAV NETWORK

Ammar Ahmed, Shuimei Zhang, and Yimin D. Zhang

Department of Electrical and Computer Engineering, Temple University, Philadelphia, PA, 19122, USA

ABSTRACT

We propose a distributed unmanned aerial vehicle (UAV) network performing collaborative radar sensing for multi-target localization and motion parameter estimation. Two UAV network topologies are considered for data propagation and information fusion. In the former, we form a sequential UAV node chain, whereas in the latter, the UAV nodes are grouped into clusters and the information among different clusters is propagated through the cluster master nodes. Sparse reconstruction methods are used to fuse the target state information from previous nodes or clusters with the data measured in the underlying nodes or clusters, depending on the adopted topology, to achieve improved target state estimates. In order to minimize the communication traffic in the UAV network, each node transmits the estimated Doppler signatures or sparse target state estimates to the next UAV node in the network or the cluster master node, in lieu of the large volume of raw sampled data. Simulation results verify the effectiveness of the proposed approaches and compare the performance between the two UAV network topologies.

Index Terms— Collaborative UAV network, target localization, motion parameter estimation, distributed radar network, passive radar.

1. INTRODUCTION

Autonomous unmanned aerial vehicles (UAVs) play a critical role in various civil, military, and homeland security applications, such as disaster monitoring, border surveillance, and relay communications [1–7]. To execute missions that are time critical or span a large geographical area, a single UAV is insufficient due to its limited energy and payload. In addition to the extended coverage, a multi-UAV network also provides diversity gain by sensing an area of interest from different aspect angles to increase the reliability of the estimated target parameters. However, the transmission and fusion of the high volume data between different UAVs pose great challenges as the UAVs are equipped with restricted on-board processing capabilities and have limited communication coverage and data transmission capacities.

The target state search space, representing the position and velocity of the targets, is sparsely populated because the targets are sparsely distributed within the surveillance area [8,9]. This fact enables sparsity-based approaches to be applied in the conventional distributed stationary radars where the Doppler frequencies observed at each radar receiver are forwarded to the global fusion center [10]. In the fusion center, the time-domain signal is reconstructed from the Doppler frequencies through the inverse discrete Fourier transform (IDFT), and the results corresponding to all receivers are fused using compressive sensing (CS) techniques, such as the complex multi-task Bayesian compressive sensing algorithm [11, 12]. However, missing or noisy samples from various nodes may result in erroneous target state estimation. In [13, 14], instantaneous target state estimates are fed to a Gaussian mixture probability hypothesis density

filter (GMPHD) to filter out the false measurements and compensate for missed detections to reduce the localization error. A feedback scheme is further introduced in [15, 16] so that the group sparse reconstruction algorithm also benefits from the *a priori* knowledge.

When considering the underlying UAV network, however, such centralized processing scheme becomes impractical because there may not be a fusion center. Even a fusion center is utilized, the UAVs have a limited communication range and thus not all of them can directly report the observed data to the fusion center. In addition, the overall communication traffic and latency would increase as the network size scales.

In this paper, we consider real-time multi-target localization and motion parameter estimation using a scalable collaborative UAV network as a passive radar utilizing the sources of opportunity [17–24]. More specifically, we consider the following functionalities: Sensing, transmission, information fusion, target localization, and motion parameter estimation. We exploit CS-based information fusion at UAVs to fuse the information captured from neighbouring nodes or neighbouring clusters with their own measurements to achieve improved target localization and motion parameter estimation. Due to the space limitation, our focus is on the CS-based network information fusion for these purposes, whereas the tracking performance incorporating the GMPHD filters will be considered separately.

Notations. A lower (upper) case bold letter denotes a vector (matrix) and $(\cdot)^{\mathrm{T}}$ represents the transpose operator. In addition, $\|\cdot\|_1$ and $\|\cdot\|_2$ express the vector l_1 and l_2 norms, respectively.
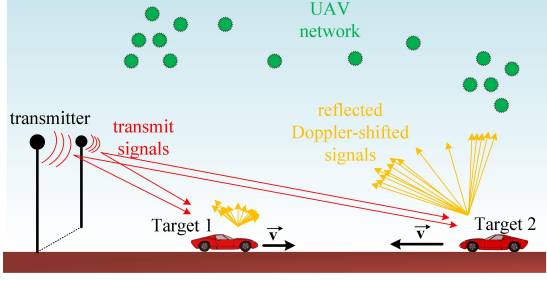
2. SYSTEM AND SIGNAL MODELS

2.1. System Geometry

Consider a collaborative UAV network consisting of N distributed UAV nodes as illustrated in Fig. 1. The mission of the UAV network is to localize multiple ground moving targets and estimate their motion parameters through the measurement and processing of the target Doppler frequencies observed at these UAVs. We assume M stationary transmitters from sources of opportunity and their locations in the three-dimensional space and the operating frequencies, respectively denoted as $\mathbf{p}_{m,\mathrm{tx}}$ and f_m, $m = 1, \cdots, M$, are known at each UAV. The location and the instantaneous velocity of the nth UAV at the time instant t are respectively denoted by $\mathbf{p}_{n,\mathrm{rx}}(t)$ and $\mathbf{v}_{n,\mathrm{rx}}(t)$, $n = 1, \cdots, N$, and are assumed known to the UAVs within its communication coverage. We assume G point targets in the sensing area of the UAV network where the gth target is located at $\mathbf{p}_{g,\mathrm{tar}}(t)$ moving with an instantaneous velocity $\mathbf{v}_{g,\mathrm{tar}}(t)$, $g = 1, \cdots, G$. The number of the targets as well as their respective positions and velocities are unknown to the UAVs.

2.2. Doppler Frequencies

Assuming proper processing of ground clutter suppression through e.g., space-time adaptive processing [25, 26] or displacement phase

Fig. 1. Passive multi-static radar exploiting a collaborative multi-UAV network.

(a) Chain network topology   (b) Clustered network topology

Fig. 2. Topological examples of the collaborative multi-UAV network.

center antenna [27], the Doppler frequencies associated with the motion of the targets and the UAV nodes can be measured at the UAVs. The bistatic instantaneous Doppler frequency of the qth target measured at the nth UAV node corresponding to the signals transmitted by the mth transmitter can be expressed as [8, 10]:

$$f_{m,n,g}(t) = -\left[\frac{\mathbf{v}_{g,\mathrm{tar}}(t) - \mathbf{v}_{n,\mathrm{rx}}(t)}{\lambda_m}\right]^{\mathrm{T}} \left[\frac{\mathbf{p}_{g,\mathrm{tar}}(t) - \mathbf{p}_{n,\mathrm{rx}}(t)}{\|\mathbf{p}_{g,\mathrm{tar}}(t) - \mathbf{p}_{n,\mathrm{rx}}(t)\|}\right] \\ - \frac{\mathbf{v}_{g,\mathrm{tar}}^{\mathrm{T}}(t)}{\lambda_m}\left[\frac{\mathbf{p}_{g,\mathrm{tar}}(t) - \mathbf{p}_{m,\mathrm{tx}}}{\|\mathbf{p}_{g,\mathrm{tar}}(t) - \mathbf{p}_{m,\mathrm{tx}}\|}\right],$$

(1)

where $\lambda_m = c/f_m$ is the wavelength of the signal transmitted by the mth transmitter, and c is the velocity of propagation of radio waves in the free space. In the sequel, we omit the notation (t) in $f_{m,n,g}(t)$ as the Doppler frequencies are considered constant during the short processing interval.

3. DOPPLER FREQUENCY ESTIMATION AT UAV NODES

For the waveform transmitted by the mth transmitter, reflected by the gth target, and received at the nth UAV node, the noise-free received slow-time signal can be expressed in the following discrete-time baseband form:

$$y_{m,n,g}(k) = \alpha_{m,n,g} e^{j(2\pi f_{m,n,g} k\delta + \phi_{m,n,g})},$$

(2)

where k is the slow-time index and δ is the slow-time interval in processing the continuous signals from the sources of opportunity in the passive radar [28]. In addition, $\alpha_{m,n,g}$ denotes the radar cross section (RCS) including the propagation attenuation, and $\phi_{m,n,g}$ is the random phase delay. The aggregated received signal at the nth UAV node takes the following form:

$$y_n(k) = \sum_{m=1}^{M}\sum_{g=1}^{G} \alpha_{m,n,g} e^{j(2\pi f_{m,n,g} k\delta + \phi_{m,n,g})} + w_n(k), \quad (3)$$

where $w_n(k)$ is the additive white Gaussian noise. High-resolution Doppler frequency estimation at each node is achieved by exploiting CS-based methods on the received data vector $\mathbf{y}_n(k) = [y_n(k), y_n(k-1), \cdots, y_n(k-K+1)]^{\mathrm{T}}$, where K is the number of slow-time samples used to estimate the Doppler frequencies. The Doppler frequency estimation can be executed at an individual UAV node by exploiting the LASSO [29] optimization as:

$$\min_{\mathbf{z}(k)} \frac{1}{2}\|\mathbf{y}_n(k) - \mathbf{W}\mathbf{z}(k)\|_2 + \mu\|\mathbf{z}(k)\|_1, \quad (4)$$

where $\mathbf{W}$ is the $K \times L$ IDFT matrix, $\mathbf{z}(k)$ is an $L \times 1$ sparse vector representing the search space of the Doppler frequencies, and $\mu > 0$ is the regularization parameter.
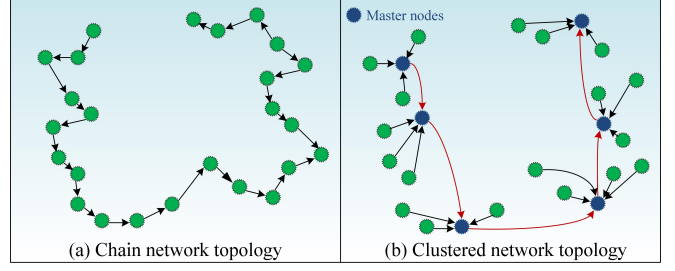
4. INFORMATION PROPAGATION AND FUSION OVER UAV NETWORK

4.1. Information Propagation

While CS-based multi-static radar approaches were developed in a global fusion manner, we extend the results to a distributed fashion to perform information propagation and fusion in the underlying collaborative multi-UAV network. As such, the UAV network is modeled as a directed graph denoted by $\mathcal{G} = (\mathcal{U}, \mathcal{W})$, where $\mathcal{U} = \{u_1, u_2, \cdots, u_n\}$ and $\mathcal{W} \subseteq (\mathcal{V} \times \mathcal{V})$ are, respectively, the set of UAV nodes and the set of edges which directionally connect the UAV nodes together as a network. The directed edge denoted by an ordered pair $w_{i,j} = (u_i, u_j)$ means a path through which node i passes information to node j. The complete directed network is the collection of all available directed edges of $w_{i,j} \in \mathcal{W}$.

We consider two network graph topologies for information propagation and data fusion as depicted in Fig. 2. In the first scenario, we follow a chained network topology, as shown in Fig. 2(a), where the Doppler information is forwarded to the subsequent node in the UAV network, i.e., $\mathcal{W} = \{w_{1,2}, w_{2,3}, \cdots w_{N-1,N}\}$. Upon receiving the Doppler information from a certain number of neighboring UAV nodes, a UAV node processes the data and generates a coarse target state estimate and passes it to the next UAV node in the network chain. In the second scenario as shown in Fig. 2(b), we utilize the clustered network topology where each node in the cluster transmits the Doppler estimates to the cluster master node. The cluster master nodes follow the chain network topology to propagate the target state estimates from one cluster master node to the other. Denote $k^{(r)} = 1^{(r)}, \cdots, Q^{(r)}$ as the kth node in the rth cluster, with $Q^{(r)}$ denoting its cluster master node. Then, the directed edges in the first cluster are denoted as $\mathcal{W}_1 = \{w_{1^{(1)},Q^{(1)}}, \cdots, w_{(Q-1)^{(1)},Q^{(1)}}\}$, whereas the directed edges in the rth cluster for $r \geq 2$ are given as $\mathcal{W}_r = \{w_{1^{(r)},Q^{(r)}}, \cdots, w_{(Q-1)^{(r)},Q^{(r)}}, w_{Q^{(r-1)},Q^{(r)}}\}$.

The information fusion and target localization for these two topologies are respectively considered in the following two subsections.

4.2. Information Fusion and Target Localization in the Chained Network Topology

Denote $\tilde{Q}$ as the minimum number of UAV nodes required to obtain the initial estimate of the sparse target scene. That is, when the Doppler measurements are collected in a UAV from fewer than $\tilde{Q}$ UAV nodes, the estimated Doppler frequencies at each node will be passed to the next UAV node in the network. On the other hand, when the Doppler frequency measurements from $\tilde{Q}$ UAV nodes are collected, the UAV will perform CS-based target position and velocity estimation. Subsequently, only the estimated target state, instead

of the estimated Doppler frequencies or sampled data, is passed to the subsequent UAV node so that the data traffic does not increase with the size of the UAV network. This strategy also enables distributed computing in an effective sequential manner.

In the sensing process, each node estimates the target Doppler frequencies from the received time sequence $\mathbf{y}_n(k)$ using Eq. (4). Once the $\tilde{Q}$th UAV node receives the estimated Doppler frequencies from the other $\tilde{Q} - 1$ UAV nodes, it creates a hypothetical data for each of the $\tilde{Q}$ nodes as follows:

$$\tilde{\mathbf{y}}_n(k) = [\tilde{y}_n(k), \tilde{y}_n(k-1), \cdots, \tilde{y}_n(k-K+1)]^{\mathrm{T}}, \quad (5)$$

with

$$\tilde{y}_n(k) = \sum_{m=1}^{M} \sum_{g=1}^{G} e^{j2\pi \hat{f}_{m,n,g} k \delta}, \quad (6)$$

where $n = 1, 2, \cdots, \tilde{Q}$, $\hat{f}_{m,n,g}$ denotes the estimated Doppler frequencies, $\tilde{y}_n(k)$ is the hypothetical data corresponding to the time sequence sampled at the nth UAV node, whereas $\tilde{\mathbf{y}}_n(k)$ is the corresponding $K \times 1$ data vector for the nth UAV node. The target localization and motion parameter estimation can be performed by employing the processed Doppler frequency data from the first $\tilde{Q}$ UAV nodes in the network through the following LASSO optimization [10]:

$$\hat{\mathbf{u}}_{\tilde{Q}}(k) = \arg \min_{\mathbf{u}_{\tilde{Q}}(k)} \frac{1}{2} \left\| \bar{\mathbf{y}}_{\tilde{Q}}(k) - \mathbf{\Psi}_{\tilde{Q}} \mathbf{u}_{\tilde{Q}}(k) \right\|_2 + \mu \left\| \mathbf{u}_{\tilde{Q}}(k) \right\|_1, \quad (7)$$

where $\bar{\mathbf{y}}_{\tilde{Q}}(k) = [\tilde{\mathbf{y}}_1^{\mathrm{T}}(k), \tilde{\mathbf{y}}_2^{\mathrm{T}}(k), \cdots, \tilde{\mathbf{y}}_{\tilde{Q}-1}^{\mathrm{T}}(k), \tilde{\mathbf{y}}_{\tilde{Q}}^{\mathrm{T}}(k)]^{\mathrm{T}}$ is the $K\tilde{Q} \times 1$ vector developed by concatenating $\tilde{\mathbf{y}}_n(k)$ for the $\tilde{Q}$ nodes using Eq. (5). Moreover, $\mathbf{\Psi}_{\tilde{Q}}$ is the $K\tilde{Q} \times L$ dictionary matrix whose columns correspond to the target locations and the respective velocities. Each column of the dictionary matrix is constructed for a specific target position and velocity using Eq. (5) by exploiting the Doppler frequencies generated by Eq. (1) for that target velocity and location. Moreover, $\mathbf{u}_{\tilde{Q}}(k)$ is the $L \times 1$ sparse vector corresponding to the respective target positions and velocities. The target positions and velocities can be defined in either a two-dimensional or three-dimensional space, depending on the geometries and the knowledge of the ground scene. In this paper, we consider a two-dimensional space.

The processed location and velocity information contained in $\mathbf{u}_{\tilde{Q}}(k)$, estimated by the optimization in Eq. (7) using $\tilde{Q}$ UAV nodes, is forwarded to the next node in the wireless network for information fusion. There are different ways to fuse data in the CS framework. In this paper, we exploit the re-weighted l_1 minimization approach [30] that modifies the LASSO with weighting factors applied to the sparse entries.

Consider the nth node with $n > \tilde{Q} - 1$. Denoting $\hat{\mathbf{u}}_{n-1}(k)$ as the target state information received from the previous node in the chain, the nth UAV node can fuse the information $\hat{\mathbf{u}}_{n-1}(k)$ with its own sampled Doppler frequency data $\mathbf{y}_n(k)$ to achieve enhanced location and velocity estimates as:

$$\hat{\mathbf{u}}_n(k) = \arg \min_{\mathbf{u}_n(k)} \frac{1}{2} \left\| \mathbf{y}_n(k) - \mathbf{\Psi}_n \mathbf{u}_n(k) \right\|_2 + \mu \left\| \mathbf{\Phi} \mathbf{u}_n(k) \right\|_1, \quad (8)$$

where $\mathbf{\Psi}_n$ is the $K \times L$ dictionary matrix whose columns correspond to the target locations and velocities, and $\mathbf{\Phi}$ is the re-weighted diagonal matrix whose ith diagonal entry is defined as:

$$[\mathbf{\Phi}]_{i,i} = \min \left[\frac{1}{|\hat{u}_{n-1}^i(k)|^\gamma}, \Omega \right], \quad (9)$$

where $\hat{u}_{n-1}^i(k)$ is the ith element of vector $\hat{\mathbf{u}}_{n-1}(k)$, γ is the weighting parameter, and Ω is a sufficiently large real value. At the last node in the UAV network, the sparse vector $\mathbf{u}_N(k)$ provides the final estimates of target positions and velocities. At the last node in the UAV network, the sparse vector $\hat{\mathbf{u}}_N(k)$ obtained using Eq. (9) provides the final estimates of target positions and velocities.

It is noted in Eq. (9) that, depending on several factors, such as the slow-time sampling interval and the network size, the sampling time of different UAV nodes can be different. As such, the target state information passed between different nodes may need to be aligned. Denote t_n and t_{n-1} as the sampling instants at the nth and the $n-1$ nodes, we can align the target state information for target g, $g = 1, \cdots, G$, using the following expression:

$$\begin{bmatrix} \mathbf{p}_{g,\mathrm{tar}}(t_n) \\ \mathbf{v}_{g,\mathrm{tar}}(t_n) \end{bmatrix} = \begin{bmatrix} \mathbf{I}_2 & (n_t - n_{t-1})\mathbf{I}_2 \\ \mathbf{0}_2 & \mathbf{I}_2 \end{bmatrix} \begin{bmatrix} \mathbf{p}_{g,\mathrm{tar}}(t_{n-1}) \\ \mathbf{v}_{g,\mathrm{tar}}(t_{n-1}) \end{bmatrix}, \quad (10)$$

where $\mathbf{I}_2$ and $\mathbf{0}_2$ represent the 2×2 identity and null matrices, respectively. These target state parameters are mapped to vectors $\mathbf{u}_n$ and $\mathbf{u}_{n-1}$.

4.3. Target Localization in Clustered Network Topology

Denote R as the total number of clusters and there are $Q^{(r)}$ UAV nodes in the rth cluster. Each UAV node estimates the Doppler frequencies using the optimization in Eq. (4) and transmits the estimated Doppler frequency information to their respective cluster master nodes.

Consider the UAV nodes $n = 1, 2, \cdots, Q^{(1)}$ in the first cluster, where the $Q^{(1)}$th node is the cluster master node. Similar to the chained network structure as described in Section 4.2, the cluster master node creates the $L \times 1$ hypothetical data vector as corresponding to the data received at each node under its jurisdiction using Eq. (5). The information from all the $Q^{(1)}$ UAV nodes can then be fused with the sampled data at the cluster master node to initiate the sensing operation as:

$$\hat{\mathbf{u}}^{(1)}(k) = \arg \min_{\mathbf{u}^{(1)}(k)} \frac{1}{2} \left\| \bar{\mathbf{y}}^{(1)}(k) - \mathbf{\Psi}^{(1)} \mathbf{u}^{(1)}(k) \right\|_2 + \mu \left\| \mathbf{u}^{(1)}(k) \right\|_1, \quad (11)$$

where $\bar{\mathbf{y}}^{(1)}(k) = [\tilde{\mathbf{y}}_1^{\mathrm{T}}(k), \tilde{\mathbf{y}}_2^{\mathrm{T}}(k), \cdots, \tilde{\mathbf{y}}_{Q^{(1)}}^{\mathrm{T}}(k)]^{\mathrm{T}}$ is the $KQ^{(1)} \times 1$ data vector, $\mathbf{\Psi}^{(1)}$ is the $KQ^{(1)} \times L$ dictionary matrix, and $\hat{\mathbf{u}}^{(1)}(k)$ is the $L \times 1$ sparse vector corresponding to the positions and velocities of the targets. The cluster master node passes the estimated $\hat{\mathbf{u}}^{(1)}(k)$ to the master node of the second cluster ($r = 2$) in the network chain of cluster master nodes.

Once the master node of the rth cluster, $r = 2, \cdots, R$, receives the estimated target state from the master node of the $(r-1)$th cluster, it can fuse the received information with the Doppler frequency estimates from the $Q^{(r)}$ UAV nodes under its jurisdiction as:

$$\hat{\mathbf{u}}^{(r)}(k) = \arg \min_{\mathbf{u}^{(r)}(k)} \frac{1}{2} \left\| \bar{\mathbf{y}}^{(r)}(k) - \mathbf{\Psi}^{(r)} \mathbf{u}^{(r)}(k) \right\|_2 \\ + \mu \left\| \mathbf{\Phi}^{(r)} u^{(r)}(k) \right\|_1, \quad (12)$$

where matrix $\mathbf{\Phi}^{(r)}$ is similarly defined as:

$$[\mathbf{\Phi}^{(r)}]_{i,i} = \min \left[\frac{1}{|\hat{u}^{(r-1),i}(k)|^\gamma}, \Omega \right], \quad (13)$$

with $\hat{u}^{(r-1),i}(k)$ denoting the ith element of $\hat{\mathbf{u}}^{(r-1)}(k)$. For the last cluster master node in the network, $\hat{\mathbf{u}}^{(R)}(k)$ provides the estimated location and velocity information of the targets.
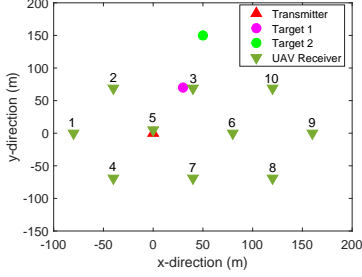
Fig. 3. The UAV network configuration.

5. SIMULATION RESULTS

We consider a collaborative UAV network consisting of 10 UAVs as shown in Fig. 3. All the UAVs are moving with the same constant speed of $[12, 0, 0]$ m/s at the height of 200 m. One illuminator located at the origin is considered which emits Digital Video Broadcasting-Terrestrial (DVB-T) signals with a carrier frequency of 950 MHz. There are two ground targets which are initially located at $[30, 70, 0]$ m and $[50, 150, 0]$ m, respectively, and move with the respective velocities of $[-7, -5, 0]$ m/s and $[-3, 3, 0]$ m/s. We assume a unit noise power, and the input signal magnitude corresponding to both targets is about 0.2, yielding an input signal-to-noise (SNR) of -14 dB. By taking advantages of the previous target states, the simulation focuses on a small search area with a size of 200 m $\times$ 200 m and velocity space between -10 m/s to 10 m/s in each direction. 10 samples are used in each dimension, yielding a grid size of $10,000$ entries. In addition, we assume $\gamma = 1$ and $\Omega = 10,000$.

In the chained network topology, we assume the minimum number of nodes to perform the initial target state estimation to be $\tilde{Q} = 5$. Each of the first four nodes estimates the Doppler frequencies using Eq. (4), and the two dominant Doppler frequency estimates are transmitted to the next UAV node. The 5th node reconstructs the sampled data using Eq. (5) and exploits the optimization in Eq. (7) to estimate the target locations and velocities. The location and motion parameter estimates are then transferred in a serial fashion to the next nodes until we reach the final node.

The estimated target state of the chained network topology is shown in Fig. 4. Fig. 4(a) depicts the results obtained in the 5th UAV node, whereas Fig. 4(b) through Fig. 4(f) show the respective results obtained at the 6th UAV through the 10th UAV. We notice that the two true peaks cannot be determined in Fig. 4(a), since the second highest peak does not associate with one of the two targets. However, with the estimated target state passing through the UAV nodes in the chained network topology, false peaks become less significant as successive information fusion taking place in the UAV network. However, the target magnitude of the second target is much lower than the true value.

For the clustered network topology, we assume that the UAV nodes 1 to 5 and 6 to 10 belong to the first and second clusters, respectively. UAV nodes 5 and 10 act as the cluster master nodes. Fig. 5(a) presents the estimated target state from the first cluster and the result is the same as in Fig. 4(a). In the second cluster, the master node 10 fuses the results from first cluster with the Doppler estimates gathered from the UAV nodes in the second cluster. Fig. 5(b) represents the results achieved after the information fusion from both clusters based on Eq. (12). It shows accurate target state estimation with much closer target magnitudes.

From 100 independent Monte Carlo trials, the root mean square error (RMSE) of the estimated target locations using the chained
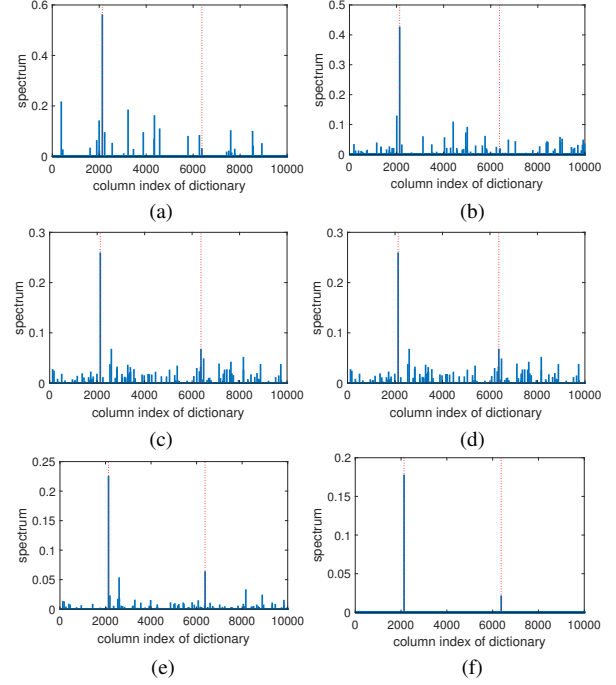

Fig. 4. Estimated target state for the chained network topology: (a) from the data observed at the first 5 nodes; (b)–(e) based on the fused data at the 6th node through the 10th node, respectively.
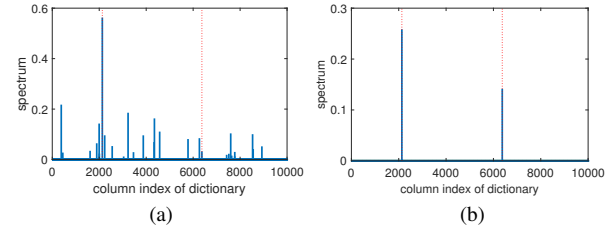

Fig. 5. Estimated sparse vector representing the target motion parameters for the clustered network topology: (a) estimated from the first cluster; (b) fused results for the first and second clusters.

network topology is 9.33 m and the RMSE of the estimated velocity is 0.97 m/s. For the clustered network topology, the obtained RMSE of the estimated target locations is 0.42 m and that of the estimated target velocity is 0.03 m/s. Overall, target state information fusion in the clustered network topology provides better performance as compared to the chained network topology.

6. CONCLUSIONS

In this paper, we proposed a multi-target motion parameter estimation method for collaborative UAV networks. In order to reduce the communication burden of transmitting a high volume of raw measurement data, the UAV nodes process the received signals and only transmit the estimated Doppler signatures to the UAV nodes in the sequence of the network chain. Two network topologies are considered to fuse the information captured from the UAV nodes to extract the improved target state estimates. Simulation results illustrate the effectiveness of the proposed approaches and compare the two types of UAV network topologies.

7. REFERENCES

[1] A. Ryan, M. Zennaro, A. Howell, R. Sengupta, and J. Hedrick, "An overview of emerging results in cooperative UAV control," in *Proc. IEEE Conf. Decision and Control*, Nassau, Bahamas, May 2004, pp. 602–607.

[2] R. C. Palat, A. Annamalai, and J. H. Reed, "Cooperative relaying for ad hoc ground networks using swarms," in *Proc. IEEE Milit. Comm. Conf.*, Atlantic City, NJ, Nov. 2005, pp. 1588–1594.

[3] D. Cole, A. Goktogan, P. Thompson, and S. Sukkarieh, "Mapping and tracking," *IEEE Robot. Autom. Mag.*, vol. 16, no. 2, pp. 22–34, June 2009.

[4] X. Li and Y. D. Zhang, "Multi-source cooperative communications using multiple small relay UAVs," in *Proc. IEEE Globecom Workshop on Wireless Networking for Unmanned Aerial Vehicles*, Miami, FL, Dec. 2010, pp. 1805–1810.

[5] B. K. Chalise, Y. D. Zhang, and M. G. Amin, "Multi-beam scheduling for unmanned aerial vehicle networks," in *Proc. IEEE/CIC Int. Conf. Commun. in China*, Xian, China, Aug. 2013, pp. 442–447.

[6] S. Hayat, E. Yanmaz, and R. Muzaffar, "Survey on unmanned aerial vehicle networks for civil applications: A communications viewpoint," *IEEE Commun. Surveys Tut.*, vol. 18, no. 4, pp. 2624–2661, 2016.

[7] E. Yanmaz, S. Yahyanejad, B. Rinner, H. Hellwagner, and C. Bettstetter, "Drone networks: Communications, coordination, and sensing," *Ad Hoc Networks*, vol. 68, pp. 1–15, Jan. 2018.

[8] Y. D. Zhang and B. Himed, "Moving target parameter estimation and SFN ghost rejection in multi-static passive radar," in *Proc. IEEE Radar Conf.*, Ottawa, Canada, April 2013, pp. 1–5.

[9] Y. D. Zhang, M. G. Amin, and B. Himed, "Structure-aware sparse reconstruction and applications to passive multi-static radar," *IEEE Aerosp. Electron. Syst. Mag.*, vol. 32, no. 2, pp. 68–78, Feb. 2017.

[10] S. Subedi, Y. D. Zhang, M. G. Amin, and B. Himed, "Group sparsity based multi-target tracking in passive multi-static radar systems using Doppler-only measurements," *IEEE Trans. Signal Process.*, vol. 64, no. 14, pp. 3619–3634, July 2016.

[11] S. Ji, D. Dunson, and L. Carin, "Multi-task compressive sensing, *IEEE Trans. Signal Process.*, vol. 57, no. 1, pp. 92–106, Jan. 2009.

[12] Q. Wu, Y. D. Zhang, M. G. Amin, and B. Himed, "Complex multitask Bayesian compressive sensing," in *Proc. IEEE Int. Conf. Acoust., Speech, Signal Process.*, Florence, Italy, May 2014, pp. 3375–3379.

[13] B. N. Vo and W. K. Ma, "The Gaussian mixture probability hypothesis density filter," *IEEE Trans. Signal Process.*, vol. 54, pp. 4091–4104, Nov. 2006.

[14] F. Yang, H. Chen, and K. Liu, "A collaborative GMPHD filter for fast multi-target tracking," in *Proc. Int. Conf. Unmanned Aircraft Systems*, Dever, CO, June 2015, pp. 559–566.

[15] S. Subedi, Y. D. Zhang, and M. G. Amin, "Sparse reconstruction of multi-component Doppler signature exploiting target dynamics," in *Proc. IEEE Int. Workshop on Comput. Adv. Multi-Sensor Adaptive Process.*, Cancun, Mexico, Dec. 2015, pp. 73–76.

[16] S. Subedi, Y. D. Zhang, M. G. Amin, and B. Himed, "Cramer-Rao type bounds for sparsity-aware multi-sensor multi-target tracking," *Signal Process.*, vol. 145, pp. 68–77, Jan. 2018.

[17] M. Malanowski and K. Kulpa, "Two methods for target localization in multistatic passive radar," *IEEE Trans. Aerosp. Electron. Syst.*, vol. 48, no. 1, pp. 572-580, Jan. 2012

[18] A. Noroozi and M. A. Sebt, "Target localization from bistatic range measurements in multi-transmitter multi-receiver passive radar, *IEEE Signal Process. Lett.*, vol. 22, no. 12, pp. 2445–2449, Dec. 2015.

[19] S. Subedi, Y. D. Zhang, M. G. Amin, and B. Himed, "Motion parameters estimation of multiple ground moving targets in multi-static passive radar systems," *EURASIP J. Adv. Signal Process.*, vol. 2014, no. 157, pp. 1–14, Oct. 2014.

[20] B. K. Chalise, Y. D. Zhang, M. G. Amin, and B. Himed, "Target localization in a multi-static passive radar system through convex optimization," *Signal Process.*, vol. 102, pp. 207–215, Sept. 2014.

[21] S. Oh, "A scalable multi-target tracking algorithm for wireless sensor networks," *Int. J. Distrib. Sensor Netw.*, vol. 8, no. 9, pp. 1–16, Sept. 2012.

[22] R. P. S. Mahler, "Multitarget Bayes filtering via first-order multitarget moments," *IEEE Trans. Aerosp. Electron. Syst.*, vol. 39, pp. 1152-1178, Oct. 2003.

[23] H. Godrich, A. M. Haimovich, and R. S. Blum, "Target localization accuracy gain in MIMO radar based system," *IEEE Trans. Inf. Theory*, vol. 56, no. 6, pp. 2783–2803, June 2010.

[24] A. Ahmed, Y. D. Zhang, and B. Himed, "Distributed dual-function radar-communication MIMO system with optimized resource allocation," in *Proc. IEEE Radar Conference*, Boston, MA, April 2019.

[25] Q. Wu, Y. D. Zhang, M. G. Amin, and B. Himed, "Space-time adaptive processing and motion parameter estimation in multistatic passive radar using sparse Bayesian learning," *IEEE Trans. Geoscience and Remote Sensing*, vol. 54, no. 2, pp. 944–957, Feb. 2016.

[26] Y. Gu and Y. D. Zhang, "Atomic decomposition-based sparse recovery for space-time adaptive processing," in *Proc. Asilomar Conf. Signals, Systems, Computers*, Pacific Grove, CA, Oct. 2018.

[27] B. Dawidowicz, K. S. Kulpa, M. Malanowski, J. Misiurewicz, P. Samczynski, and M. Smolarczyk, "DPCA detection of moving targets in airborne passive radar," *IEEE Trans. Aerosp. Electron. Syst.*, vol. 48, no. 2, pp. 1347–1357, April 2012.

[28] C. Berger, B. Demissie, J. Heckenbach, P. Willett, and S. Zhou, "Signal Processing for Passive Radar Using OFDM Waveforms," *IEEE J. Selected Topics in Signal Process.*, vol. 4, no. 1, pp. 226–238, Feb. 2010.

[29] R. Tibshirani, "Regression shrinkage and selection via the lasso," *J. R. Stat. Soc. Series B Stat. Methodol.*, vol. 58, no. 1, pp. 267–288, 1996.

[30] E. J. Candés, M. B. Wakin, and S. P. Boyd, "Enhancing sparsity by reweighted l-1 minimization," *J. Fourier Anal. Appl.*, vol. 14, no. 5–6, pp. 877–905, Dec. 2008.